



Mechanistic Kinetic Analysis of Fast Pyrolysis of Vanillin to Primary Phenols

Attada Yerrayya, Upendra Natarajan and Ravikrishnan Vinu*

Department of Chemical Engineering, Indian Institute of Technology Madras, Chennai, India

Vanillin is a major fine chemical in the flavoring industry and one of the pyrolysates from lignin. In order to understand the primary decomposition pathways of vanillin, analytical fast pyrolysis experiments were performed in the temperature range of 500°C–650°C, and the primary pyrolysates were quantified. The proposed pyrolysis chemistry involves 31 elementary reactions of 23 species. Thermodynamic and kinetic analyses were performed using quantum chemical density functional theory calculations. Reaction pathways for the formation of three major phenolics, viz., guaiacol, 5-formylsalicylaldehyde and 4-hydroxybenzaldehyde, that accounted for ~80 wt% yield at 650°C, were proposed. Based on the bond dissociation energies (BDEs) of homolytic cleavage of the various bonds in vanillin, the primary reaction is shown to involve the cleavage of O–CH₃ bond whose BDE is 61.4 kcal mol⁻¹. New bimolecular reactions such as ipso-addition involving the reaction of vanillin with hydrogen and methyl radicals were proposed. The generation of 4-hydroxy methoxybenzyl radical was found to be vital for the formation of guaiacol, while 4-hydroxy-3-(λ³-methoxyl) benzaldehyde radical was the key intermediate for the formation of 5-formylsalicylaldehyde. Multiple pathways for the formation of guaiacol, 5-formylsalicylaldehyde, catechol and 4-hydroxybenzaldehyde were evaluated. In order to track the time evolution of vanillin and its major pyrolysates, a detailed kinetic model was developed using the elementary reactions and their Arrhenius rate parameters. Based on the kinetic model, it is inferred that the timescale of fast pyrolysis is captured well by the model.

OPEN ACCESS

Edited by:

Nanda Kishore,
Indian Institute of Technology
Guwahati, India

Reviewed by:

Alberto Roldan,
Cardiff University, United Kingdom
Anjani Ravi Kiran Gollakota,
National Yunlin University of Science
and Technology, Taiwan

*Correspondence:

Ravikrishnan Vinu
vinu@iitm.ac.in

Specialty section:

This article was submitted to
Bioenergy and Biofuels,
a section of the journal
Frontiers in Energy Research

Received: 29 March 2022

Accepted: 01 June 2022

Published: 13 July 2022

Citation:

Yerrayya A, Natarajan U and Vinu R
(2022) Mechanistic Kinetic Analysis of
Fast Pyrolysis of Vanillin to
Primary Phenols.
Front. Energy Res. 10:907505.
doi: 10.3389/fenrg.2022.907505

Keywords: vanillin, pyrolysis, kinetics, rate parameter, density functional theory (DFT)

INTRODUCTION

Haarmann and Reimer (Pinto et al., 2012) first produced vanillin from petroleum-based guaiacol in late 1800s. Synthetic vanillin was produced using lignin-containing waste generated from pulp and paper industries between 1930s and 1980s. Currently, vanillin produced from guaiacol accounts for 85% of the world supply. However, lignin is a very attractive feedstock for the production of vanillin owing to feedstock sustainability. Vanillin has been used extensively as a flavoring and fragrance ingredient in the food industry, as an additive in cosmetic industry, as a chemical precursor in the synthesis of pharmaceuticals, and as a reactant for second generation platform chemicals (Pacek et al., 2013). Approximately, 20,000 tons of vanillin are produced every year, of which only 3,000 tons is obtained from lignin (Holladay et al., 2007; Silva et al., 2009). Owing to the rich aromatic functionality of lignin, it is foreseen as a promising feedstock for vanillin production (Daugsch and Pastore, 2005; Fache et al., 2015). Vanillin is one of the major pyrolysis products from lignin, formed by the cleavage of β-O-4 and α-O-4 linkages (Lou et al., 2010), and importantly, vanillin contains different functional groups such as hydroxyl, formyl and methoxyl groups, which are very common

in the macromolecular structure of lignin. The mechanism of pyrolysis of lignin is complex, and the formation of phenolics and aromatic hydrocarbons from lignin involves a number of competing elementary reactions and pathways. This is also exacerbated by the variation in pyrolysis operating conditions like heating rate, reaction/residence time and temperature.

Lignin model compounds like monomeric and dimeric phenols find value in fundamental studies that attempt to build a step-by-step and comprehensive understanding of lignin fast pyrolysis. Establishing the pyrolysis pathways of the monomeric phenols is imperative to understand their gas phase pyrolysis and cracking, which becomes important at high pyrolysis severities, i.e., at high temperatures and longer residence times. Some studies have investigated the fast pyrolysis mechanism of lignin monomeric model compounds such as catechol (Asmadi et al., 2011a), guaiacol (Dorrestijn and Mulder, 1999; Huang et al., 2013a; Liu et al., 2014; Yerrayya et al., 2019), syringol (Huang et al., 2013b) and vanillin (Britt et al., 2000; Shin et al., 2001; Asmadi et al., 2011b; Liu et al., 2016; Wang et al., 2016). Wang et al. (2016) reported that the initial step in thermal decomposition of vanillin is the homolytic cleavage of O-CH₃ bond. Concerted reactions are dominant at high temperatures due to the high activation energy. It is reported that hydrogen abstraction reactions are the major propagation reactions for the formation of products from pyrolysis of vanillin. Britt et al. (2000) investigated the fast pyrolysis of vanillin, and found that guaiacol was the main product at low temperatures, while salicylaldehyde was the dominant product at higher temperatures (600°C–700°C). This means that the conversion of methoxy group to aldehyde group occurs through radical-induced rearrangement of the methoxy group at elevated temperatures (Britt et al., 2000; Asmadi et al., 2011a). Shin et al. (2001) investigated the fast pyrolysis of vanillin using molecular beam mass spectrometry to detect gas phase products. The experiments were conducted in a spiral quartz tube inside a straight quartz tube in the temperature range of 500°C–800°C, and residence time of 0.3–0.6 s. They found that the conversion of vanillin is low at 500°C, while complete conversion occurred at 650°C. The main products from vanillin pyrolysis were catechol, 4-hydroxybenzaldehyde, guaiacol, 3,4-dihydroxybenzaldehyde, 5-formylsalicylaldehyde at 650°C. Further, they observed the formation of aromatic compounds such as benzene, naphthalene, and anthracene at 800°C. Liu et al. (2016) studied the pyrolysis of three different guaiacyl type monomeric compounds, viz., vanillin, vanillic acid and vanillyl alcohol, using density functional theory (DFT) approach. They reported that the major products from vanillin in the temperature range of 400°C–600°C were guaiacol and 5-formylsalicylaldehyde, while at high temperatures, other products like 2-hydroxybenzaldehyde, 1,2-benzenediol, 2-methylphenol and 2-ethylphenol were observed.

This study is unique as it unifies analytical fast pyrolysis experiments, quantum chemical DFT calculations and microkinetic modeling to unravel the key reaction pathways and kinetics of formation of guaiacol, 5-formylsalicylaldehyde, and 4-hydroxybenzaldehyde from vanillin. New pathways for the formation of guaiacol and 4-hydroxybenzaldehyde *via* ipso-

addition reaction of vanillin with hydrogen radical, and a bimolecular reaction of vanillin with methyl radical are proposed, and their kinetics are investigated for the first time. The kinetic model results are discussed, especially from the viewpoint of the time scale of product evolution and the major reaction pathways for the formation of the key products.

EXPERIMENTAL AND COMPUTATIONAL DETAILS

Experimental Details

Analytical fast pyrolysis experiments were performed in a single shot micropyrolyzer (PY-3030S, Frontier Laboratories, Japan), and the evolved pyrolysates were analyzed using a gas chromatograph/mass spectrometer (GC/MS, Shimadzu GC-2010/QP2010 Plus). The schematic of the micropyrolyzer-GC/MS set-up is available elsewhere (Yerrayya et al., 2019). In a typical experiment, 320 ± 30 µg of vanillin (99% purity, Sigma Aldrich) was taken in a deactivated stainless-steel sample cup, and dropped into the micropyrolyzer tube that was set at the desired temperature (500°C–650°C). The typical heating rate experienced by solid biomass samples like cellulose is reported to be 200°C s⁻¹ (Proano-Aviles et al., 2017), which can be categorized as fast heating. Vanillin is expected to be heated to the pyrolysis temperature within a few seconds (1–2 s), as it is a liquid at ambient conditions. The evolved pyrolysates were separated in a UA-5 capillary column (30 m length × 0.25 mm i.d. × 0.25 µm film thickness). Ultra-high pure helium (99.9995% purity) was used as the carrier gas at 1.0 ml min⁻¹ with a split ratio of 14.3:1. The injector, interface and MS ion source temperatures were set at 300°C, 300°C and 250°C, respectively. The GC oven temperature program was set as follows: 40°C for 1 min followed by a ramp at 10°C min⁻¹ to 280°C, and finally held for 10 min at 280°C. The electron ionization voltage was 70 eV, and the pyrolysates were scanned in the m/z range of 50–500 Da. The mass spectra of the individual compounds were compared with NIST and Wiley libraries to identify the organic compounds. The identified compounds had match factor > 90%. The major compounds, viz., vanillin, guaiacol, 5-formylsalicylaldehyde and 4-hydroxybenzaldehyde, were calibrated using pure compound standards to determine their absolute wt% yields. The calibration plot between mass and peak area of the standard compounds resulted in a straight line with zero intercept and high correlation coefficient (R² ≈ 0.99). All the experiments were repeated in triplicate to determine the standard deviations in the yield and selectivity of the products, and these are reported in the tables and figures.

Computational Details

The equilibrium geometries of the reactants, intermediates, transition states and products were optimized using dispersion parameterized functional (M06-2X) developed by the Truhlar group and 6-31++G (d, p) basis set, with the Gaussian 09 software package (Frisch et al., 2016). This functional gives an excellent performance for thermochemistry, non-covalent interactions and kinetics calculations with an average error of 1.3 kcal mol⁻¹ (Zhao

and Truhlar, 2008). Optimization and vibrational frequency calculations were performed using the (opt + freq) keyword, and transition state calculations were performed using the (opt = TS) freq keyword in Gaussian. In order to optimize the geometry, a quasi-Newtonian optimization method was employed and the tolerance was set at 10^{-6} . The selection of the basis set depends on the type of molecule and system size. For large systems, a smaller basis set might suffice, because of the trade-off between accuracy and computational time (Davidson and Feller, 1986).

The reactants, intermediates and products were fully optimized followed by frequency calculations to verify the stationary points on the potential energy surface (PES). The vibrational spectrum of a transition state is characterized by one imaginary frequency (implying a negative force constant), which means that in one direction in the nuclear configuration space, the energy is maximum, and in all other (orthogonal) directions the energy is minimum. There is only one very large imaginary frequency that describes the bond-forming and bond-breaking processes. Typically, the bends and rotations caused by anharmonicities are characterized by less than 100 cm^{-1} frequency, which is usually negligible for transition state structures. Thus, the first order saddle points were identified as stationary points with single imaginary frequency. Molecular structures of reactants, intermediates, transition states, and products, and vibrational frequencies were visualized, and analyzed using Gaussview 5.0 (Dennington et al., 2009). Bond dissociation energy (BDE) was calculated using Eq. 1:

$$BDE (\text{kcal mol}^{-1}) = H_{298} (R) + H_{298} (X) - H_{298} (R - X) \quad (1)$$

where, $H (R)$, $H (X)$ and $H (R-X)$ refer to the enthalpy of product radicals R and X, and the reactant, R-X, which involved zero-point energy, respectively, at 298.15 K and 1 atm. For the homolytic cleavage reactions, the activation energies were assumed to be the same as the BDEs (Huang et al., 2011). The Gaussian calculations involving BDE, enthalpy change and entropy change associated with a reaction were also calculated at different temperatures. For the propagation reactions, the Gibbs free energies corresponding to the activated complex were calculated using the keyword “temperature” in the geometry script.

The transition state theory (TST), used to determine the rate constants of the elementary propagation reactions (k_{TST}), is given by:

$$k_{TST} = \frac{k_B T}{h} \exp\left(\frac{-\Delta G^\ddagger}{RT}\right) \quad (2)$$

where k_B , T , h , and R denote the Boltzmann constant, temperature, Planck's constant and universal gas constant, respectively. ΔG^\ddagger refers to the Gibbs free energy change associated with the activated complex or transition state with respect to the reactant. This is given by $\Delta G^\ddagger = \Delta H^\ddagger - T\Delta S^\ddagger$; where ΔH^\ddagger and ΔS^\ddagger denote the enthalpy and entropy change associated with the activated complex, respectively. The value of R at standard conditions is taken as $1.98 \times 10^{-3} \text{ kcal mol}^{-1} \text{ K}^{-1}$. The enthalpy, entropy and Gibbs free energy changes associated with the transition state were determined as the difference between the energies or entropy of the transition

state and that of the reactants. Equilibrium relationship, given by $\Delta G^0 = -RT \ln (K_{eq})$, was employed to determine the rate constant of the backward reactions in reversible reaction steps. In this relationship, ΔG^0 refers to the reaction Gibbs free energy change at standard condition, while K_{eq} is the equilibrium constant given by the ratio of forward to backward rate constant ($k_{forward}/k_{backward}$). Linearized form of Arrhenius equation, $\ln (k_{TST}) = \ln A - E_a/RT$, was used to determine the activation energy (E_a) and pre-exponential factor (A) of the elementary steps. In order to determine the time evolution of species concentrations during fast pyrolysis, the estimated rate parameters were used in a kinetic model, which contained the species balance equations for all the reactants, products and intermediates. The rate of change of concentration of a species (P) is simply the sum of all the rates of change of all elementary reaction steps in which species P takes part:

$$\frac{d[P]_j}{dt} = \sum_i \nu_{ij} r_i \quad (3)$$

Where r_i is the rate of reaction of elementary reaction step, i , and ν_{ij} is the stoichiometric coefficient of species j in reaction i . As per the usual convention, the stoichiometric coefficient is negative when the species is consumed in a specific reaction, while it is positive when it is generated. The rate equations are available in **Supplementary Material**. The non-linear set of ordinary differential equations (ODEs) were solved using the ODE15s sub-routine of Matlab® 2017a (Jain et al., 2012) without applying pseudo steady state approximation on the free radical and short-lived intermediates. ODE15s is a variable step continuous implicit solver based on the backward differentiation and the numerical differentiation formulae of the Gear's first order implicit method. This method can be used for backward differentiation of orders 1 to 5 and stiff differential equations (Celaya et al., 2014). The initial concentration of vanillin was 1 mol L^{-1} , while that of all other species were zero.

RESULTS AND DISCUSSION

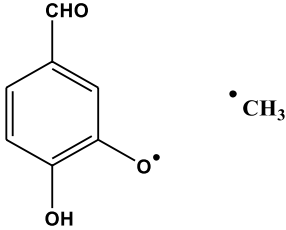
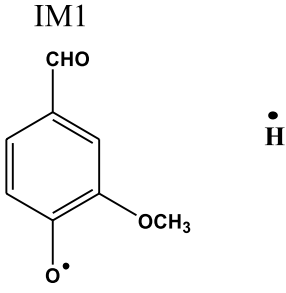
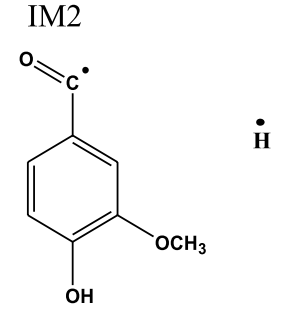
Analytical Fast Pyrolysis of Vanillin

Fast pyrolysis experiments were performed at different temperatures, viz., 500°C , 550°C , 600°C and 650°C . The composition of phenolics obtained from vanillin are summarized in **Table 1**. The top three compounds in the phenolic fraction include guaiacol, 5-formylsalicylaldehyde and 4-hydroxybenzaldehyde. The conversion of vanillin to volatile organics followed the trend: $69.3\% (650^\circ\text{C}) > 39.8\% (600^\circ\text{C}) > 19.2\% (550^\circ\text{C}) > 8.3\% (500^\circ\text{C})$. Guaiacol is the major pyrolysate from vanillin, and its formation involves the removal of formyl group. The second major product is 5-formylsalicylaldehyde, which is formed by the rearrangement of O-CH_3 , while retaining the formyl group of vanillin. The other major product is 4-hydroxybenzaldehyde, which is formed by the removal of methoxy group from vanillin. Other phenolic compounds such as 2-ethylphenol, 2-methoxy-4-methylphenol, 3-methoxybenzaldehyde, 1,2-benzendiol, and 2-hydroxybenzaldehyde were detected at 650°C , albeit at low

TABLE 1 | List of phenolic compounds obtained from fast pyrolysis of vanillin at different temperatures, and their composition (in peak area%). The wt% yields of major species are shown in parenthesis.

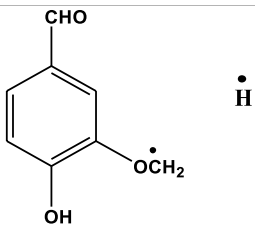
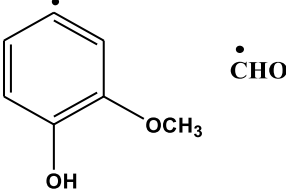
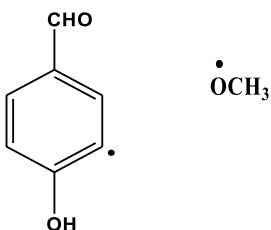
	500°C	550°C	600°C	650°C
Benzaldehyde, 4-hydroxy-	0 (0)	0 (0)	1.7 (3.1 ± 1.7)	5.4 (13.1 ± 1.3)
Phenol, 2-methoxy- (Guaiacol)	0.1 (0)	6.7 (12.2 ± 1.5)	14.2 (30.7 ± 1.9)	16.4 (44.9 ± 2.7)
5-Formylsalicylaldehyde	0 (0)	1.5 (2 ± 0.3)	6.5 (9.8 ± 1.9)	11.9 (22.7 ± 2.0)
Phenol, 2-ethyl-	0	0	0	0.3
Phenol, 2-methoxy-4-methyl-	0	0	0.1	0.3
Benzaldehyde, 2,3-dihydroxy-	0	0	0	0.2
Benzaldehyde, 3-methoxy-	0	0	0	0.3
1,3-Benzenedimethanol	0	0	0	0.4
Phenol, 2-ethyl-4-methyl-	0	0	0	0.1
Catechol	0	0	0	3.2
Phenol-2-methoxy-4-vinyl-	0	0.1	0.5	0.5
Benzaldehyde, 2-hydroxy-	0	0	0	7.4
4-Hydroxy-3-methylbenzaldehyde	0	0	0.9	3.1
3-Methyl-p-anisaldehyde	0	0	2.0	3.3
Benzene, 1-hydroxy-2-methoxy-4-methyl-	0	0	0	0.6

TABLE 2 | Comparison of bond dissociation energies (in kcal mol⁻¹) of vanillin from this study and the literature values calculated using different methods.

Products	M06-2X/6-31++G (d, p) (this study)	M06-2X/6-311+G (d, p) Pelucchi et al. (2019)	CBS-4M Hu et al. (2016)	B3LYP/cc-PVDZ Shin et al. (2001)
 IM0	61.4	61.2	61	65
 IM1	88.1	87.5	90	87
 IM2	89.0	94.0	88	88
IM3				

(Continued on following page)

TABLE 2 | (Continued) Comparison of bond dissociation energies (in kcal mol⁻¹) of vanillin from this study and the literature values calculated using different methods.

Products	M06-2X/6-31++G (d, p) (this study)	M06-2X/6-311+G (d, p) Pelucchi et al. (2019)	CBS-4M Hu et al. (2016)	B3LYP/cc-PVDZ Shin et al. (2001)
 IM5	97.2	97.4	100	94
 IM7	102.1	102.0	104	91
 IM4	104.8	104.3	109	102

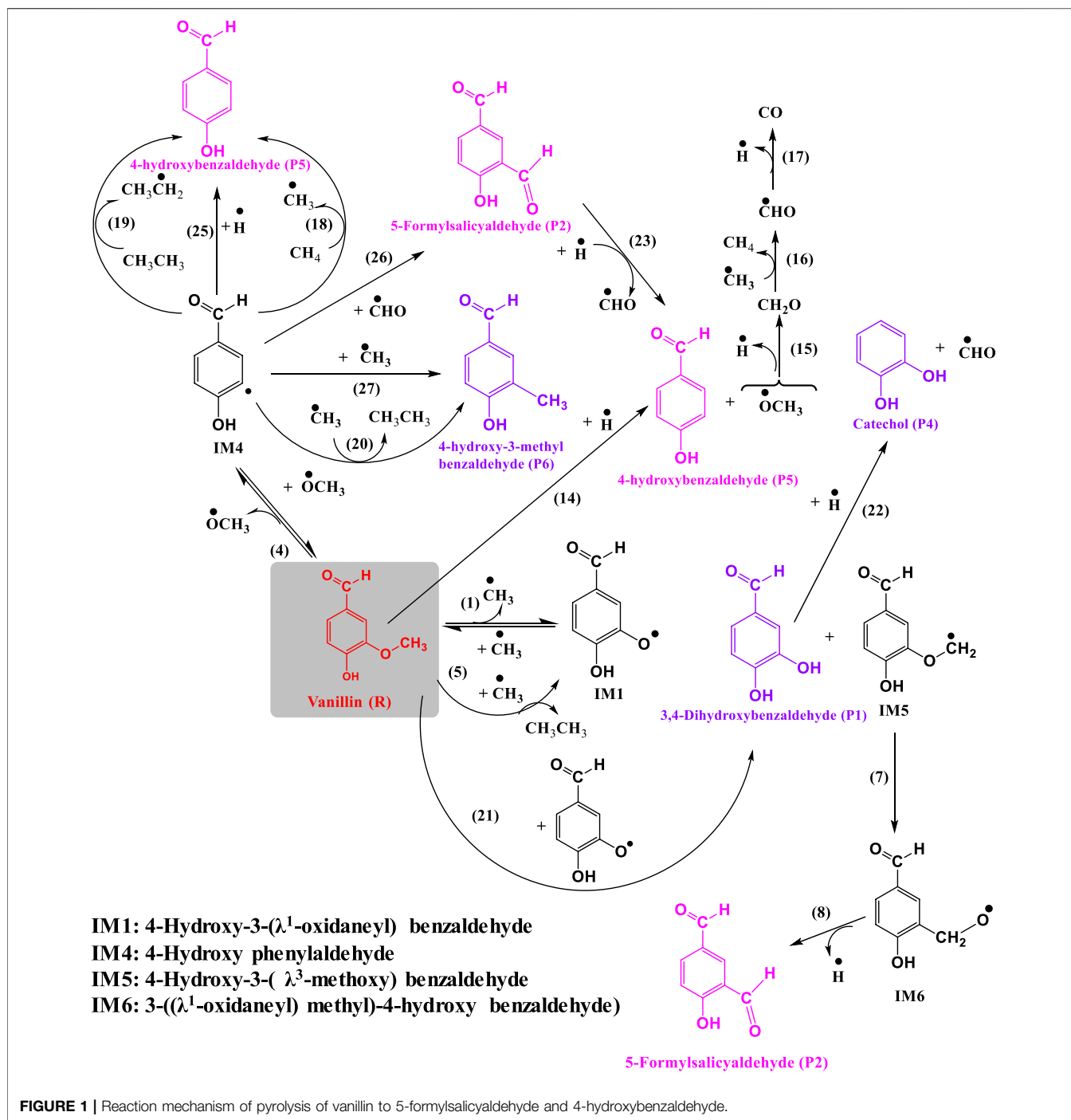
The full names of the free radicals (IM1, IM2, IM3, IM4, IM5, IM7) are available in **Figures 1, 2**.

relative peak area%. The formation of 3-methoxybenzaldehyde involves the removal of hydroxyl group of vanillin, and this requires high temperature because of the high bond dissociation energy of C_{aromatic}-OH bond, which is discussed in the next section. At high temperatures, the formation of 1,2-benzendiol is observed due to the secondary decomposition of guaiacol. In addition to phenolic compounds, a few non-phenolic aromatics and linear chain alkenes were produced, albeit at low GC/MS peak area% (<4%).

Mechanism of Transformation of Vanillin

According to Egawa et al. (2006) and Velcheva and Stamboliyska (2004), the difference in energy between the trans and cis conformers of vanillin is very small (1.1 kcal mol⁻¹). Therefore, no specific distinction is made between the two conformers in this study. **Table 2** depicts the major products from homolytic cleavage of various bonds of vanillin, and the corresponding BDEs. These initiation reactions involve the cleavage of (a) O-C_{aliphatic}, (b) O-H, (c) C-H of formyl group, (d) CH₂-H of

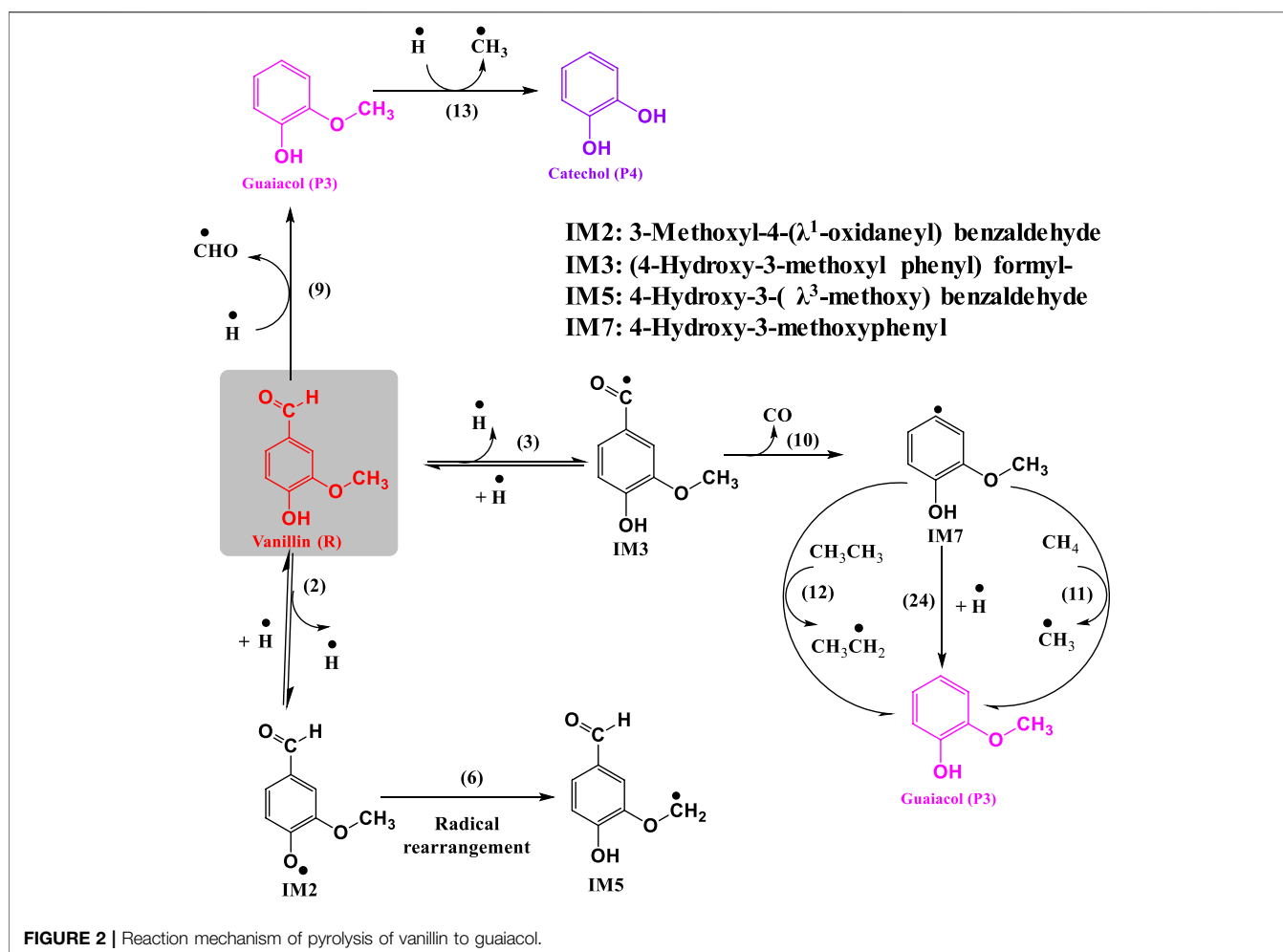
methyl group, (e) C_{aromatic}-OCH₃, and (f) C_{aromatic}-CHO, and lead to the formation of free radicals such as methyl, hydrogen, methoxy, and formyl. The BDEs follow the trend: O-CH₃ (61.4 kcal mol⁻¹) < O-H (88.1 kcal mol⁻¹) < C-H of formyl group (89.0 kcal mol⁻¹) < CH₂-H methyl group (97.2 kcal mol⁻¹) < C_{aromatic}-CHO (102.1 kcal mol⁻¹) < C_{aromatic}-OCH₃ (104.8 kcal mol⁻¹). Comparison of BDEs of vanillin calculated in this study, and those reported by Pelucchi et al. (2019), Shin et al. (2001) and Hu et al. (2016) are presented in **Table 2**. The key differences between these three studies involve the method and the basis set used. Pelucchi et al. (2019) used a very similar method as ours, viz., M06-2X/6-311+g (d, p), while Shin et al. (2001) used B3LYP/cc-PVDZ, and Hu et al. (2016) used CBS-4M. In general, the BDEs calculated using higher level methods like M06-2X and CBS-4M agree with each other, whereas the B3LYP functional fails to estimate the correct energies for some reactions. The BDE values for most of reactions are in close agreement with Pelucchi et al. (2019), and Hu et al. (2016). Verma and Kishore (2017) used B3LYP functional and a



similar basis set as ours [6-311+g (d, p)], and reported BDEs that are similar to this study for most of the bond types. However, the B3LYP functional seems to underestimate the BDEs for O-CH₃ and C_{aromatic}-OCH₃. Based on the order of BDEs, it can be concluded that the primary bond fission or initiation process involves the homolytic cleavage of O-CH₃ bond to form 4-hydroxy-3-(λ^1 -oxidanyl) benzaldehyde (IM1) and methyl radical. The homolytic cleavage of O-H and C-H are

competitive reactions, which result in the generation of 3-methoxy-4-(λ^1 -oxidanyl) benzaldehyde (IM2) and hydrogen radical, and (4-hydroxy-3-methoxy phenyl)-methaneone (IM3) and hydrogen radicals, respectively.

Figures 1, 2 depict the elementary reactions involved in vanillin pyrolysis, as proposed in this study. In total, there are 31 elementary reactions of 23 different species including free radicals and stable species. The optimized structures of all



the 23 species, and their geometries, including bond lengths, bond angles and dihedral angles, are available in **Supplementary Material**. The elementary reactions can be grouped into specific reaction families such as bond fission, propagation (H-abstraction, radical rearrangement, ipso-addition, β -scission), and radical recombination. The forward reactions of (1)-(4) denote the free radical initiation reactions involving bond fission, reactions (5)-(23) are of propagation type, and reactions (24)-(27) and the reverse reactions of (1)-(4), i.e., reactions (28)-(31), involve free radical recombination.

Following the homolytic cleavage of O-CH₃ to produce IM1 and methyl radical, the fission of O-H, C_{formyl}-H and C_{aromatic}-OCH₃ occur *via* reactions (2), (3), and (4), respectively. These reactions, respectively, generate 3-methoxy-4-(λ^1 -oxidaneyl) benzaldehyde (IM2) and hydrogen radical, (4-hydroxy-3-methoxy phenyl)-methaneone (IM3) and hydrogen radical, and 4-hydroxy benzylaldehyde (IM4) and methoxy radical. For bond fission reactions, the activation energy was calculated by using the values of the enthalpy of the reaction (or BDE) and temperature using the relationship, $E_a = \Delta H^0 - RT$. This is especially valid for homolytic reactions because the transition state is close to the energy level of the products, and

according to the structure-activity relationship of Evans-Polanyi, the activation energy is similar to the BDE. The pre-exponential factor (A) for bond fission reactions, which is in the range of 10^{15} - 10^{17} s⁻¹, was taken from the literature reported by Vinu and Broadbelt (2012). Eyring-Polanyi equation was used for calculating the rate constants. Radical recombination reactions are much faster than other types of reactions, and therefore, activation energies are negligible. The rate parameters of all the elementary reactions are listed in **Table 3**.

Table 3 and **Figure 1** depict a number of propagation steps, which include unimolecular scission reactions that result in the formation of a free radical and a stable species, and bimolecular reactions between a stable species and a free radical. Reaction (5) involves the reaction of vanillin (R) molecule with methyl radical to form the intermediate, IM1, and ethane by the removal of methyl group from vanillin. This proceeds through a transition state with activation energy of 37.8 kcal mol⁻¹. The transition state structure (TS₁) is characterized by an imaginary frequency of 1,173 cm⁻¹. The IM2 radical formed from reaction (2) can undergo intermolecular transfer to form 4-hydroxy-3-(λ^3 -methoxy) benzaldehyde radical (IM5) *via* transition state (TS₂) with activation energy of 23.2 kcal mol⁻¹. This is depicted by reaction (6). The IM5 radical can further undergo

TABLE 3 | Kinetic parameters of the elementary reactions in vanillin fast pyrolysis.

Reaction no.	Reactions	E_a (kcal mol ⁻¹)	A (s ⁻¹ or cm ³ mol ⁻¹ s ⁻¹)
1, 28	$R \xrightarrow{k_1} IM1 + \dot{C}H_3$	59.6; 0	3×10^{15} ; 1×10^{13}
2, 29	$R \xrightarrow{k_2} IM2 + \dot{H}$	86.3; 0	1×10^{16} ; 1×10^{14}
3, 30	$R \xrightarrow{k_3} IM3 + \dot{H}$	87.2; 0	5×10^{17} ; 1×10^{13}
4, 31	$R \xrightarrow{k_4} IM4 + \dot{H}$	103.0; 0	5×10^{17} ; 1×10^{13}
5	$R + \dot{C}H_3 \xrightarrow{k_5} IM1 + CH_3\dot{C}H_3$	37.8	5×10^{10}
6	$IM2 \xrightarrow{k_6} IM5$	23.2	1.6×10^{12}
7	$IM5 \xrightarrow{k_7} IM6$	8.1	1.2×10^{13}
8	$IM6 \xrightarrow{k_8} P2 + \dot{H}$	12.4	5.2×10^{12}
9	$R + \dot{H} \xrightarrow{k_9} P3 + \dot{C}HO$	8.0	2.9×10^{13}
10	$IM3 \xrightarrow{k_{10}} IM7 + CO$	26.7	7.6×10^{14}
11	$IM7 + CH_4 \xrightarrow{k_{11}} P3 + \dot{C}H_3$	7.7	1.4×10^{12}
12	$IM7 + CH_3\dot{C}H_3 \xrightarrow{k_{12}} P3 + CH_3\dot{C}H_2$	6.4	1.2×10^{12}
13	$P3 + \dot{H} \xrightarrow{k_{13}} P4 + \dot{C}H_3$	15.9	6×10^{14}
14	$R + \dot{H} \xrightarrow{k_{14}} P5 + \dot{O}CH_3$	4.0	5×10^{11}
15	$\dot{O}CH_3 \xrightarrow{k_{15}} HCHO + \dot{H}$	27.1	2.4×10^{14}
16	$HCHO + \dot{C}H_3 \xrightarrow{k_{16}} CH_4 + \dot{C}HO$	7.1	1.4×10^{12}
17	$\dot{C}HO \xrightarrow{k_{17}} CO + \dot{H}$	18.5	2.6×10^{14}
18	$IM4 + CH_4 \xrightarrow{k_{18}} P5 + \dot{C}H_3$	9.7	1.1×10^{12}
19	$IM4 + CH_3\dot{C}H_3 \xrightarrow{k_{19}} P5 + CH_3\dot{C}H_2$	10.0	5×10^{10}
20	$IM4 + CH_3CH_3 \xrightarrow{k_{20}} P6 + \dot{C}H_3$	42.4	1.6×10^{13}
21	$R + IM1 \xrightarrow{k_{21}} P1 + IM5$	19.5	5.5×10^{10}
22	$P1 + \dot{H} \xrightarrow{k_{22}} P4 + \dot{C}HO$	8.4	0.8×10^{13}
23	$P2 + \dot{H} \xrightarrow{k_{23}} P5 + \dot{C}HO$	7.7	0.6×10^{13}
24	$IM7 + \dot{H} \xrightarrow{k_{24}} P3$	0	1.0×10^{13}
25	$IM4 + \dot{H} \xrightarrow{k_{25}} P5$	0	1.0×10^{14}
26	$IM4 + \dot{C}HO \xrightarrow{k_{26}} P2$	0	1.0×10^{12}
27	$IM4 + \dot{C}H_3 \xrightarrow{k_{27}} P6$	0	1.0×10^{12}

radical rearrangement to form 3-((λ^1 -oxidaneyl) methyl)-4-hydroxy benzaldehyde (IM6) (reaction 7), and this proceeds through a transition state (TS₃) with activation energy of 8.1 kcal mol⁻¹. This reaction is endothermic and the enthalpy change of reaction is found to be 3.7 kcal mol⁻¹. IM6 radical can then undergo unimolecular decomposition to form 5-formylsalicylaldehyde (P2) and hydrogen radical through a transition state with an energy barrier of 12.4 kcal mol⁻¹, and the dehydrogenation reaction is endothermic with enthalpy of 16.2 kcal mol⁻¹. This reaction is thermodynamically non-spontaneous, and it may be spontaneous at higher temperatures. The imaginary frequency of the transition state structure (TS₄) for reaction (8) is 953 cm⁻¹, and the structure is depicted **Figure 3**.

In reaction (9), vanillin reacts with hydrogen radical to form guaiacol (P3) by the removal of aldehyde group from the molecule. This class of reaction is known as ipso addition reaction, and is shown in **Figure 2**. This reaction proceeds through a transition state with activation energy of 8.0 kcal mol⁻¹. This value is close to the value 5 kcal mol⁻¹ reported by Pelucchi et al. (2019). The difference in the calculated activation energy is due to the basis set adopted by Pelucchi et al. (2019) which is different compared to that used in

this study. The imaginary frequency of the transition state structure (TS₅) is 872 cm⁻¹. The bond length of C(1)-C(8) increases from 1.540 to 2.60 Å corresponding to the transition state. The IM3 radical formed through reaction (3) can undergo unimolecular decomposition to form 4-hydroxy-3-methoxybenzyl (IM7) and carbon monoxide (CO) *via* reaction (10) with an activation energy of 26.7 kcal mol⁻¹.

The IM7 radical formed *via* reaction (10) can react with methane and ethane to form methyl radical and ethyl radical, respectively. Reaction (11) involves the formation of guaiacol (P3) *via* H-abstraction with methane. This reaction is endothermic and the heat of reaction is calculated as 2.25 kcal mol⁻¹. It proceeds through a transition state with activation energy of 9.7 kcal mol⁻¹. A single imaginary frequency (1,416 cm⁻¹) was observed for this transition state (TS₁₂). An alternate reaction pathway for the formation of guaiacol (P3) *via* reaction (12) involves the reaction of IM7 with ethane *via* H-abstraction. This exothermic reaction proceeds with an activation energy of 8.4 kcal mol⁻¹, with an enthalpy of 7.07 kcal mol⁻¹. The imaginary frequency of the transition state structure (TS₁₄) is 1,431 cm⁻¹. Guaiacol reacts with hydrogen radical to form catechol (P4) and methyl radical

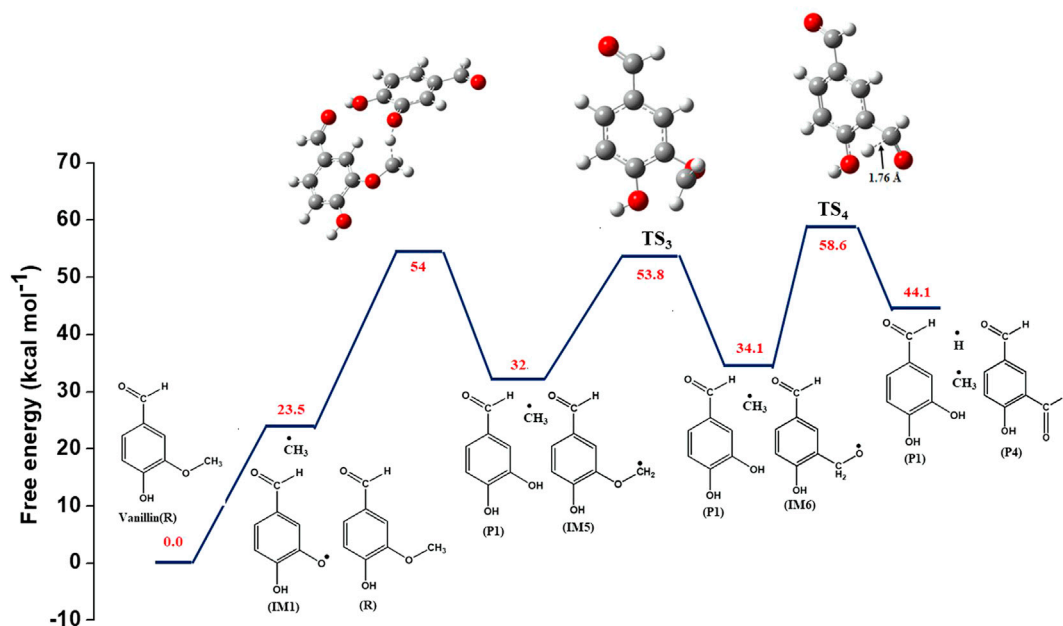


FIGURE 3 | Potential energy profile for the transformation of vanillin to 5-formylsalicylaldehyde.

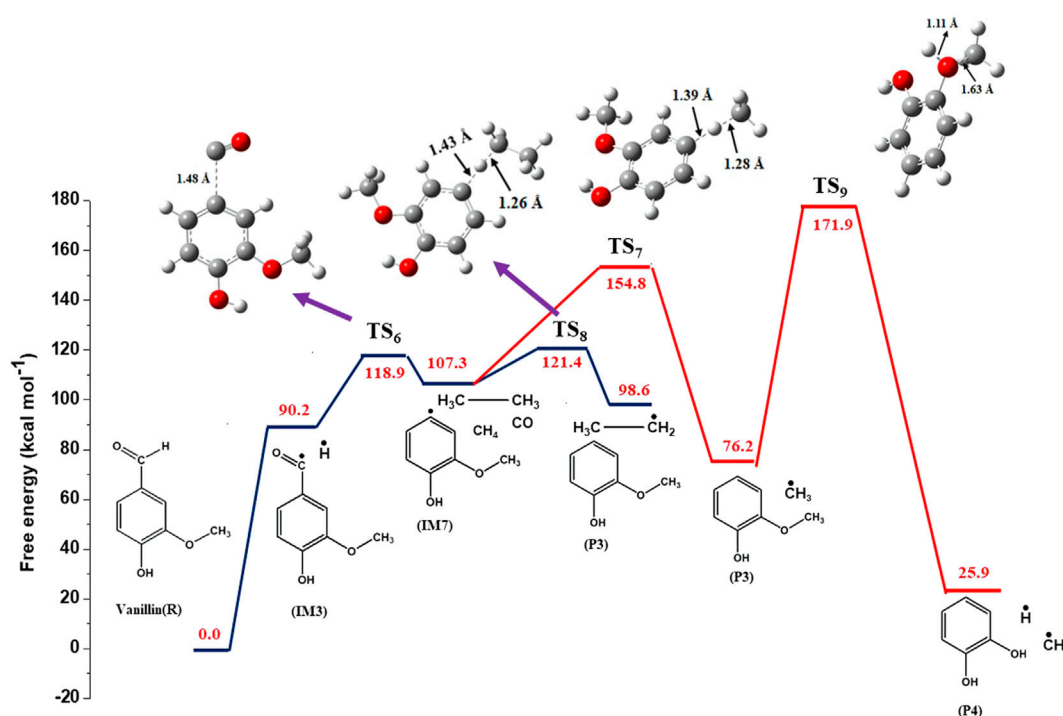


FIGURE 4 | Potential energy profile for the transformation of vanillin to guaiacol.

via transition state (TS₉) with an energy barrier of 15.9 kcal mol⁻¹. This demethylation reaction releases 13.5 kcal mol⁻¹. It can be clearly observed from the optimized

structure of TS₉ from **Figure 4** that the length of O(17)-C(12) bond is increased from 1.43 to 1.63 Å. In reaction (14), vanillin reacts with hydrogen radical to form 4-hydroxybenzaldehyde

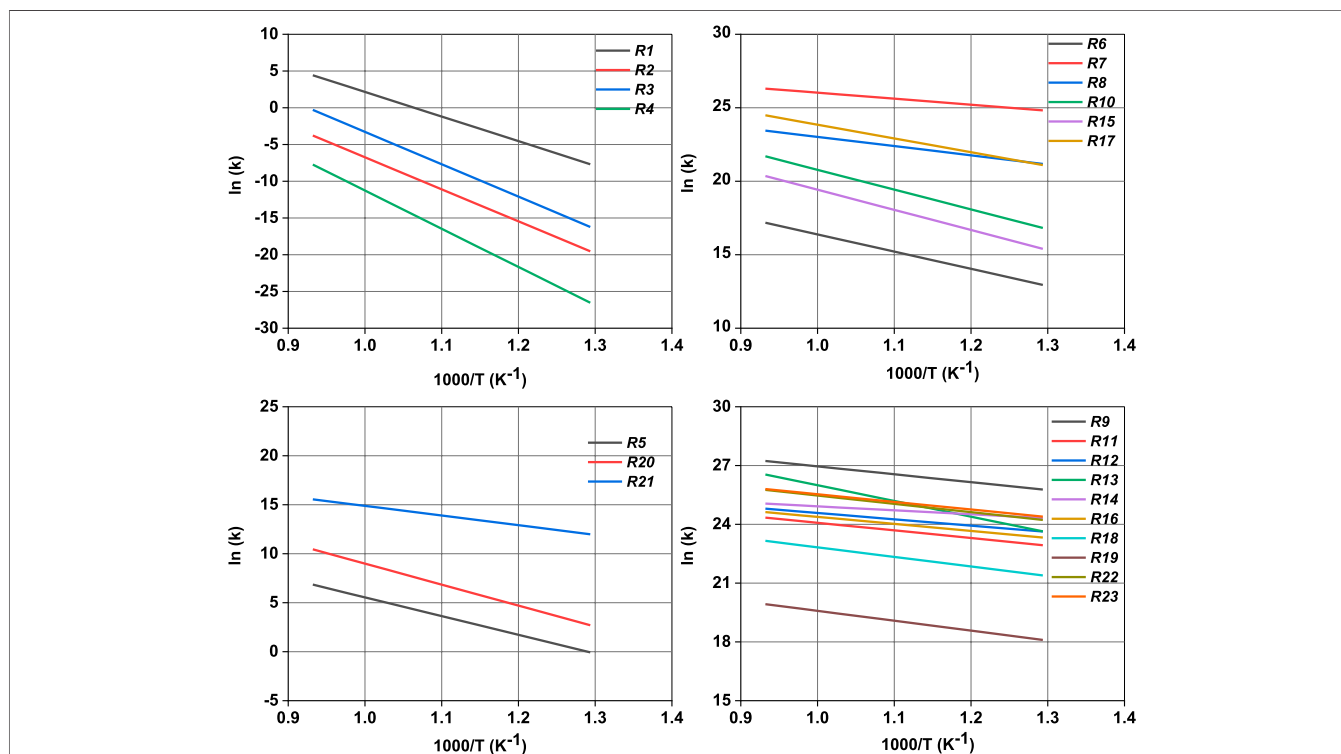
TABLE 4 | Reaction enthalpy, entropy, and Gibbs free energy calculated at 298.15 K and 1 atm using M06-2X/6-31++G (d, p) level of theory.

Reaction no.	ΔH^0 (kcal mol ⁻¹)	ΔS^0 (kcal mol ⁻¹ K ⁻¹)	ΔG^0 (kcal mol ⁻¹)
5	-33.82	-0.11	-1.01
6	9.09	0.00	9.28
7	3.71	0.01	2.12
8	16.18	0.02	9.92
9	-3.69	0.02	-8.44
10	27.71	0.04	17.13
11	2.25	0.11	-31.16
12	-7.07	0.01	-8.75
13	-13.46	0.12	-50.25
14	-6.47	0.02	-11.61
15	23.63	0.02	16.31
16	-21.74	-0.11	11.97
17	15.11	0.02	8.85
18	-3.03	0.11	-36.47
19	-12.34	0.01	-14.06
20	-8.93	0.11	-41.75
21	9.39	0.00	8.53
22	-5.32	0.01	-9.79
23	-14.00	0.01	-18.3

(P5) and methoxy radical through ipso-addition reaction involving a transition state (TS₁₀) with energy barrier of 4 kcal mol⁻¹. The exothermic ipso-addition reaction has an energy of 6.5 kcal mol⁻¹.

Shen et al. (2010) proposed that the methoxy radical is initially converted to formaldehyde, which finally forms carbon

monoxide. Based on this, the following reaction steps are proposed in this study. The unimolecular β -scission of methoxy radical leads to the formation of formaldehyde and hydrogen radical *via* reaction (15), whose activation energy is calculated to be 27.1 kcal mol⁻¹. This value is in reasonable agreement with 27.6 kcal mol⁻¹ reported in the literature (Batt, 1979). Formaldehyde further reacts with methyl radical to form methane and formyl radical *via* H-abstraction [reaction (16)]. This proceeds with an activation energy of 7.1 kcal mol⁻¹, whereas the reported E_a for this reaction is 4.9 kcal mol⁻¹ (Liu et al., 2003). The variation can be attributed to the method and basis set used by Liu et al. (2003), which was MP2/6-311G (d, p). The formyl radical then decomposes to hydrogen radical and carbon monoxide through a transition state with activation energy of 18.5 kcal mol⁻¹, given by reaction (17). This is very close to that reported in the literature (19.0 kcal mol⁻¹) for this reaction (Adams et al., 1979). The imaginary frequency of this transition state structure is 661 cm⁻¹. The intermediate IM4 formed from reaction (4) reacts with methane to form 4-hydroxybenzaldehyde (P5) and methyl radical *via* transition state (TS₁₄) with activation energy of 9.7 kcal mol⁻¹. This reaction is exothermic with reaction enthalpy of 3 kcal mol⁻¹. The length of C(17)-H(15) bond in the optimized structure of TS₁₄ increased from 0.96 to 1.28 Å. In reaction (19), IM4 reacts with ethane to form 4-hydroxybenzaldehyde (P5) and ethyl radical through the exothermic H-abstraction *via* transition state (TS₁₅) with energy barrier of 10 kcal mol⁻¹. An alternate pathway for the formation of 4-hydroxybenzaldehyde is *via*

**FIGURE 5** | Variation of rate constants of elementary steps at different pyrolysis temperatures.

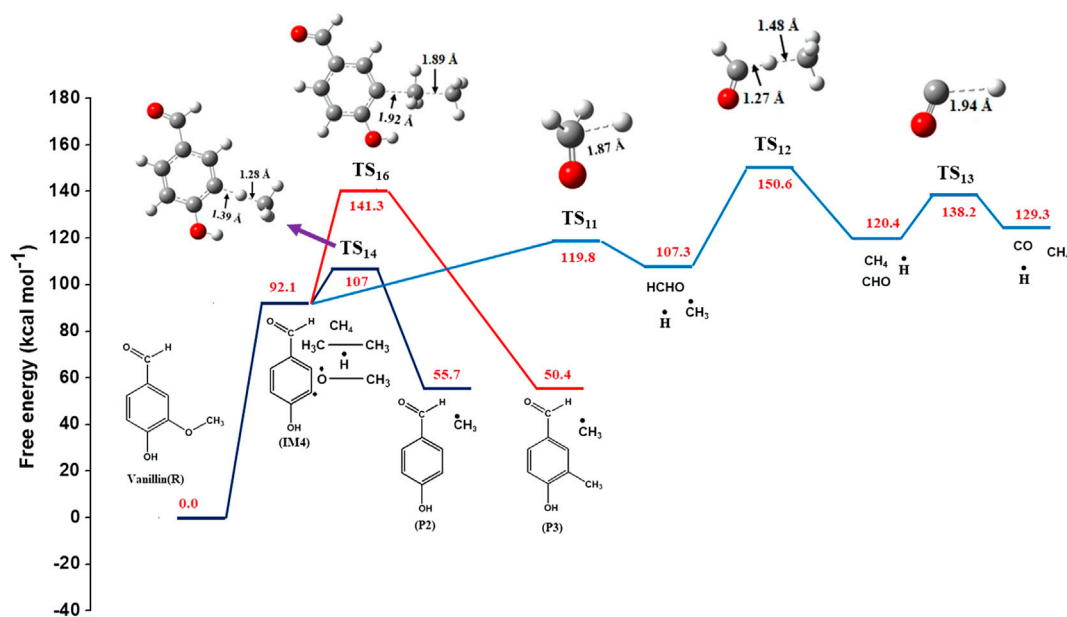


FIGURE 6 | Potential energy profile for the transformation of vanillin to 4-hydroxybenzaldehyde.

demethylation reaction (19), where IM4 reacts with ethane to form 4-hydroxy-3-methyl benzaldehyde (P6) and methyl radical. This reaction proceeds through a transition state with high energy barrier of 42.4 kcal mol⁻¹. A single imaginary frequency (1,416 cm⁻¹) was observed for this transition state (TS₁₆).

3,4-dihydroxybenzaldehyde (P1) reacts with hydrogen radical to form catechol (P4) and formyl radical *via* transition state (TS₁₇) with an energy barrier of 8.4 kcal mol⁻¹. This value is close to the literature value 5 kcal mol⁻¹ reported by Pelucchi et al. (2019). The difference in the calculated activation energy is due to the initial reactant (Salicylaldehyde) used by Pelucchi et al. (2019), which is different compared to that used in this study. The imaginary frequency of the transition state structure (TS₁₇) is 1,018 cm⁻¹. In reaction (23), 5-formylsalicylaldehyde reacts with hydrogen radical to form 4-hydroxybenzaldehyde (P5) and formyl radical through ipso-addition reaction. This exothermic reaction proceeds with an activation energy of 7.7 kcal mol⁻¹, with an enthalpy of 14 kcal mol⁻¹. The imaginary frequency of the transition state structure (TS₁₈) is 1,040 cm⁻¹.

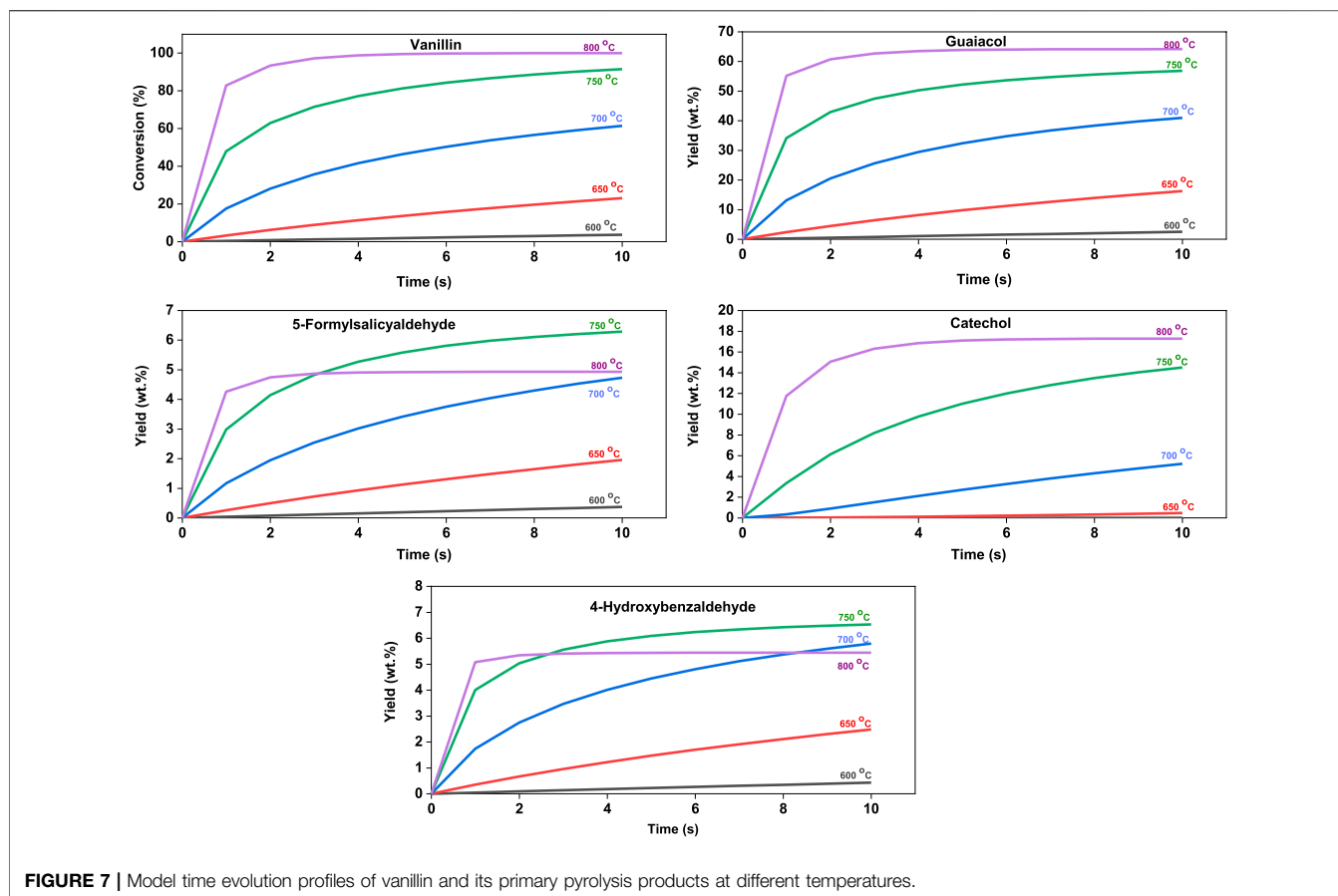
Recombination of various free radicals generated from the above-mentioned steps is important for the formation of stable products. Reactions (24), (25), (26) and (27) denote the recombination of intermediate IM7 with hydrogen radical to form guaiacol, IM4 with hydrogen radical to form 4-hydroxybenzaldehyde, IM4 with formyl radical to form 5-formylsalicylaldehyde, and IM4 with methyl radical to form 4-hydroxy-3-methyl benzaldehyde. The reversible reactions of bond fission are also of recombination type, and all these lead to the formation of vanillin.

The values of reaction enthalpy, reaction entropy and reaction Gibbs free energy are presented for all the reactions except bond fission and recombination reactions in Table 4. Figure 3 depicts

the transformation of vanillin through reactions (1), (21), (7) and (8) to 5-formylsalicylaldehyde. From Figure 5 it is seen that the rate constants of these reactions follow the trend: $k_7 > k_8 > k_{21}$. Figure 4 depicts multiple pathways involved in the formation of IM3, IM7, guaiacol and catechol. Transformation of vanillin occurs through reactions (3), (10), (11) and (13) to catechol, and reactions (3), (10) and (12) to guaiacol. Besides reactions (11) and (12), reaction (9) also leads to the formation of guaiacol in a single step. The rate constants follow the trend: $k_9 > k_{12} > k_{11} > k_{10}$ in the temperature range of interest, and this is evident from Figure 5. Therefore, reaction (10) will be least preferred, while all other reactions will be competitive. Figure 6 depicts the transformation of vanillin through reactions (4) and (18) to 4-hydroxybenzaldehyde, and reactions (4) and (20) to 4-hydroxy-3-methylbenzaldehyde. From Figure 5, it is clear that $k_{18} > k_{20}$, which shows that the production of 4-hydroxybenzaldehyde will be higher than 4-hydroxy-3-methylbenzaldehyde.

Mechanistic Kinetic Analysis

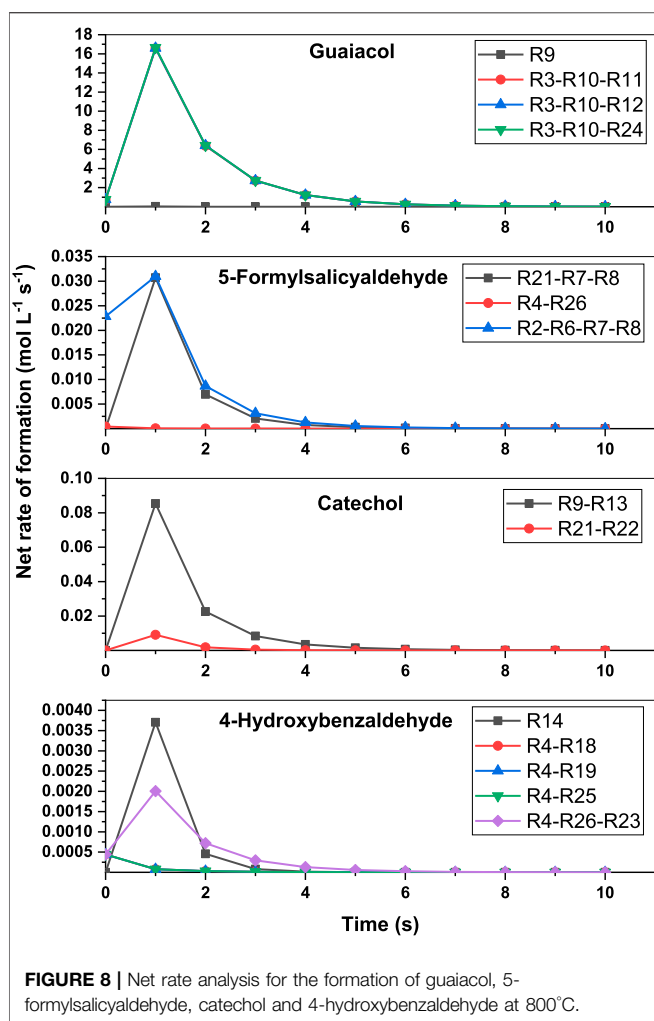
A mechanistic kinetic model was developed to understand the concentration profiles of all species involved in the reaction mechanism at different temperatures. Rate expressions were developed for all species in the reaction network. The reaction rates, described using the mass action principle, are shown in Supplementary Material. The 23 ordinary differential equations were solved simultaneously to obtain the concentration profiles. The conversion profile of vanillin and yield profiles of guaiacol, 5-formylsalicylaldehyde, catechol and 4-hydroxybenzaldehyde are shown in Figure 7. It is evident from the kinetic model that the conversion of vanillin increases with increasing temperature from 600°C to 800°C. Maximum conversion of vanillin (99.99%) was achieved at 800°C at a shorter time period (5 s). The yield of



guaiacol and catechol increased with time upto 10 s at any specific temperature, whereas the yield of 5-formylsalicylaldehyde and 4-hydroxybenzaldehyde increased upto 750°C. It is interesting to note that a decrease in final yield of 5-formylsalicylaldehyde and 4-hydroxybenzaldehyde was observed when the pyrolysis temperature is increased from 750°C to 800°C. This indicates the competing nature of the reaction pathways and the significance of rate of reactions at various temperatures. The total yield of phenolics (91.8 wt%) was found to be maximum at 800°C and 5 s. It is worthwhile to note that the time taken to reach the steady state concentration of the products is shorter as the temperature is increased. A similar observation is reported by Pelucchi et al. (2019) for vanillin pyrolysis at 500°C–800°C. They reported the lumped yields of primary, secondary and tertiary pyrolysis products from vanillin at timescales shorter than 1 s. The production of tertiary pyrolysis products is shown to occur at temperatures above 700°C. Moreover, many products like phenol, benzene, salicylaldehyde, guaiacol and 4-hydroxyisophthalaldehyde continued to evolve even after 1 s, demonstrating the complexity of vanillin pyrolysis.

In order to unravel the major pathways for the formation of products from vanillin pyrolysis, net rate analysis of the various reaction pathways was carried out. From the net rate curves depicted in Figure 8, it is evident that the net rates of the pathways R3-R10-R11, R3-R10-R12 and R3-R10-R24 are all similar, and significantly higher than that of R9, for the formation of guaiacol. This shows that

the reactions R3 and R10 are necessary for the formation of IM7, which then undergoes hydrogen abstraction reaction to form guaiacol. This is in contrast to the results of Pelucchi et al. (2019) who carried out sensitivity analysis and showed that ipso-addition reaction of vanillin with a hydrogen radical is a key pathway for the formation of guaiacol. This study shows that guaiacol formation can occur at a faster rate through a series of free radical reactions R3-R10 via intermediates IM3 and IM7. For the formation of 5-formylsalicylaldehyde, both the pathways, viz., R21-R7-R8 and R2-R6-R7-R8, are competitive owing to their similar rates. This shows that the formation of the intermediates IM5 and IM4 are key for the formation of this product. For the formation of catechol, the net rate of R9-R13 pathway is better than that of the R21-R22 pathway. This shows that catechol is mostly formed as a decomposition product of guaiacol than 3,4-dihydroxy benzaldehyde. Finally, the ipso-addition reaction, R14, is the unique pathway for the formation of 4-hydroxybenzaldehyde. Moreover, the pathway involving R4-R26-R23 is also a dominant pathway for the formation of 4-hydroxybenzaldehyde, which shows that the ipso-addition reactions are quite important for the formation of the products. However, the bimolecular recombination of IM4 with hydrogen radical or the hydrogen abstraction reactions of IM4 are not competitive for the formation of 4-hydroxybenzaldehyde. In our earlier study on guaiacol fast pyrolysis, it was shown that the inclusion of ipso-addition reactions in the kinetic model brought down the reaction time by an order of magnitude to tens of seconds, while



simultaneously affecting the yields of phenol and cresol (Yerrayya et al., 2019). In the case of vanillin pyrolysis, the time scale predicted by the model is quite similar to fast pyrolysis conditions, and this demonstrates the validity of the kinetic model. This study thus provides motivation to investigate deeper into the mechanistic aspects of pyrolysis of lignin model compounds, and develop comprehensive kinetic models to capture the formation of more by-products. It is also imperative to generate time resolved experimental data of the products in order to validate such mechanistic models.

CONCLUSION

In this work, vanillin was taken as a model lignin monomer, and the kinetics of formation of primary pyrolysis vapors are investigated using a combination of experiments, quantum chemical DFT calculations and kinetic modelling. The major

products observed from Py-GC/MS experiments include guaiacol, 5-formylsalicylaldehyde and 4-hydroxybenzaldehyde. The homolytic cleavage of O-CH₃ bond is the initial thermal decomposition step in fast pyrolysis with O-H bond cleavage being a competitive reaction. The proposed vanillin pyrolysis reaction mechanism involves four initiation, nineteen propagation and eight termination reactions. The formation of guaiacol occurs mainly through H-abstraction and ipso-addition reactions of the radicals formed from vanillin homolysis. The results show that ipso-addition reactions are predominant among all other reactions involved in the reaction chemistry for the formation of guaiacol and 4-hydroxybenzaldehyde. It is also a major reaction class that occurs at short time scales during fast pyrolysis. Kinetic analysis revealed that the radical rearrangement and β -scission reactions are dominant for the formation of 5-formylsalicylaldehyde. It can be concluded that the proposed reaction model is in reasonable agreement with the experimental time scales. It is hoped that the combined approach of experimental, theoretical and kinetic modelling will be useful for the understanding of fast pyrolysis of more complex model molecules like lignin dimers and oligomers.

DATA AVAILABILITY STATEMENT

The original contributions presented in the study are included in the article/Supplementary Materials, further inquiries can be directed to the corresponding author.

AUTHOR CONTRIBUTIONS

RV and UN conceptualized and designed the study. AY performed experiments, calculations and modeling. RV and AY developed the methodology of the study, validated the data and prepared the graphs and tables. AY wrote the first draft of the manuscript. All authors contributed to manuscript revision, read, and approved the submitted version.

ACKNOWLEDGMENTS

The authors thank P.G. Senapathy Center for providing computational resources at the Indian Institute of Technology Madras.

SUPPLEMENTARY MATERIAL

The Supplementary Material for this article can be found online at: <https://www.frontiersin.org/articles/10.3389/fenrg.2022.907505/full#supplementary-material>

REFERENCES

- Adams, G. F., Bent, G. D., Purvis, G. D., and Bartlett, R. J. (1979). The Electronic Structure of the Formyl Radical HCO. *J. Chem. Phys.* 71, 3697–3702. doi:10.1063/1.438824
- Asmadi, M., Kawamoto, H., and Saka, S. (2011a). Thermal Reactions of Guaiacol and Syringol as Lignin Model Aromatic Nuclei. *J. Anal. Appl. Pyrolysis* 92, 88–98. doi:10.1016/j.jaap.2011.04.011
- Asmadi, M., Kawamoto, H., and Saka, S. (2011b). Thermal Reactivities of Catechols/Pyrogallols and Cresols/Xylenols as Lignin Pyrolysis Intermediates. *J. Anal. Appl. Pyrolysis* 92, 76–87. doi:10.1016/j.jaap.2011.04.012
- Batt, L. (1979). The Gas-Phase Decomposition of Alkoxy Radicals. *Int. J. Chem. Kinet.* 11, 977–993. doi:10.1002/kin.550110905
- Britt, P. F., Buchanan, A. C., III, Cooney, M. J., and Martineau, D. R. (2000). Flash Vacuum Pyrolysis of Methoxy-Substituted Lignin Model Compounds. *J. Org. Chem.* 65, 1376–1389. doi:10.1021/jo991479k
- Celaya, E. A., Aguirrezabala, J. J. A., and Chatzipantelidis, P. (2014). Implementation of an Adaptive BDF2 Formula and Comparison with the MATLAB Ode15s. *Procedia Comput. Sci.* 29, 1014–1026. doi:10.1016/j.procs.2014.05.091
- Daugusch, A., and Pastore, G. (2005). Obtenção de vanilina: oportunidade biotecnológica. *Quím. Nova* 28, 642–645. doi:10.1590/s0100-40422005000400017
- Davidson, E. R., and Feller, D. (1986). Basis Set Selection for Molecular Calculations. *Chem. Rev.* 86, 681–696. doi:10.1021/cr00074a002
- Dennington, R., Keith, T., and Millam, J. (2009). *Shawnee Mission, KS, Gauss View 05*. Semichem Inc. v.5.0.9.
- Dorrestijn, E., and Mulder, P. (1999). The Radical-Induced Decomposition of 2-Methoxyphenol. *J. Chem. Soc. Perkin Trans. 2*, 777–780. doi:10.1039/a809619h
- Egawa, T., Kameyama, A., and Takeuchi, H. (2006). Structural Determination of Vanillin, Isovanillin and Ethylvanillin by Means of Gas Electron Diffraction and Theoretical Calculations. *J. Mol. Struct.* 794, 92–102. doi:10.1016/j.molstruc.2006.01.042
- Fache, M., Boutevin, B., and Caillol, S. (2015). Vanillin Production from Lignin and its Use as a Renewable Chemical. *ACS Sustain. Chem. Eng.* 4, 35–46. doi:10.1021/acssuschemeng.5b01344
- Frisch, M. J., Trucks, G. W., Schlegel, H. B., Scuseria, G. E., Robb, M. A., Cheeseman, G., et al. (2016). *Gaussian 09, Revision A.02*. Gaussian, Inc. Wallingford CT.
- Holladay, J., Bozell, J., White, J., and Johnson, D. (2007). *Top Value-Added Chemicals from Biomass Volume II-Results of Screening for Potential Candidates from Biorefinery Lignin*. PNNL-16983. Richland, WA: PNNL.
- Hu, Y., Zuo, L., Liu, J., Sun, J., and Wu, S. (2016). Chemical Simulation and Quantum Chemical Calculation of Lignin Model Compounds. *BioResources* 11, 1044–1060.
- Huang, J.-b., Liu, C., Ren, L.-r., Tong, H., Li, W.-m., and Wu, D. (2013b). Studies on Pyrolysis Mechanism of Syringol as Lignin Model Compound by Quantum Chemistry. *J. Fuel Chem. Technol.* 41, 657–666. doi:10.1016/s1872-5813(13)60031-6
- Huang, J., Li, X., Wu, D., Tong, H., and Li, W. (2013a). Theoretical Studies on Pyrolysis Mechanism of Guaiacol as Lignin Model Compound. *J. Renew. Sustain. Energy* 5, 043112. doi:10.1063/1.4816497
- Huang, X., Liu, C., Huang, J., and Li, H. (2011). Theory Studies on Pyrolysis Mechanism of Phenethyl Phenyl Ether. *Comput. Theor. Chem.* 976, 51–59. doi:10.1016/j.comptc.2011.08.001
- Jain, M. K., Iyengar, S. R. K., and Jain, R. K. (2012). *Numerical Methods*. 6th edition. New Delhi: New Age International.
- Liu, C., Deng, Y., Wu, S., Mou, H., Liang, J., and Lei, M. (2016). Study on the Pyrolysis Mechanism of Three Guaiacyl-Type Lignin Monomeric Model Compounds. *J. Anal. Appl. Pyrolysis* 118, 123–129. doi:10.1016/j.jaap.2016.01.007
- Liu, C., Zhang, Y., and Huang, X. (2014). Study of Guaiacol Pyrolysis Mechanism Based on Density Function Theory. *Fuel Process. Technol.* 123, 159–165. doi:10.1016/j.fuproc.2014.01.002
- Liu, J.-y., Li, Z.-s., Wu, J.-y., Wei, Z.-g., Zhang, G., and Sun, C.-c. (2003). Theoretical Study and Rate Constant Calculation of the CH₂O+CH₃ Reaction. *J. Chem. Phys.* 119, 7214–7221. doi:10.1063/1.1605938
- Lou, R., Wu, S.-b., and Lv, G.-j. (2010). Effect of Conditions on Fast Pyrolysis of Bamboo Lignin. *J. Anal. Appl. Pyrolysis* 89, 191–196. doi:10.1016/j.jaap.2010.08.007
- Pacek, A. W., Ding, P., Garrett, M., Sheldrake, G., and Nienow, A. W. (2013). Catalytic Conversion of Sodium Lignosulfonate to Vanillin: Engineering Aspects. Part 1. Effects of Processing Conditions on Vanillin Yield and Selectivity. *Ind. Eng. Chem. Res.* 52, 8361–8372. doi:10.1021/ie4007744
- Pelucchi, M., Cavallotti, C., Cuoci, A., Faravelli, T., Frassoldati, A., and Ranzi, E. (2019). Detailed Kinetics of Substituted Phenolic Species in Pyrolysis Bio-Oils. *React. Chem. Eng.* 4, 490–506. doi:10.1039/c8re00198g
- Proano-Aviles, J., Lindstrom, J. K., Johnston, P. A., and Brown, R. C. (2017). Heat and Mass Transfer Effects in a Furnace-Based Micropyrolyzer. *Energy Technol.* 5, 189–195. doi:10.1002/ente.201600279
- Rodrigues Pinto, P. C., Borges da Silva, E. A., and Rodrigues, A. E. (2012). Lignin as Source of Fine Chemicals: Vanillin and Syringaldehyde. *Biomass Convers.*, 381–420. Springer: New York. doi:10.1007/978-3-642-28418-2_12
- Shen, D. K., Gu, S., Luo, K. H., Wang, S. R., and Fang, M. X. (2010). The Pyrolytic Degradation of Wood-Derived Lignin from Pulping Process. *Bioresour. Technol.* 101, 6136–6146. doi:10.1016/j.biortech.2010.02.078
- Shin, E.-J., Nimlos, M. R., and Evans, R. J. (2001). A Study of the Mechanisms of Vanillin Pyrolysis by Mass Spectrometry and Multivariate Analysis. *Fuel* 80, 1689–1696. doi:10.1016/s0016-2361(01)00055-2
- Silva, E. A. B. d., Zabkova, M., Araújo, J. D., Cateto, C. A., Barreiro, M. F., Belgacem, M. N., et al. (2009). An Integrated Process to Produce Vanillin and Lignin-Based Polyurethanes from Kraft Lignin. *Chem. Eng. Res. Des.* 87, 1276–1292. doi:10.1016/j.cherd.2009.05.008
- Velcheva, E. A., and Stamboliyska, B. A. (2004). IR Spectral and Structural Changes Caused by the Conversion of 3-Methoxy-4-Hydroxybenzaldehyde (Vanillin) into the Oxyanion. *Spectrochimica Acta Part A Mol. Biomol. Spectrosc.* 60, 2013–2019. doi:10.1016/j.saa.2003.10.018
- Verma, A. M., and Kishore, N. (2017). Molecular Modelling Approach to Elucidate the Thermal Decomposition Routes of Vanillin. *New J. Chem.* 41, 8845–8859. doi:10.1039/c7nj02004j
- Vinu, R., and Broadbelt, L. J. (2012). Unraveling Reaction Pathways and Specifying Reaction Kinetics for Complex Systems. *Annu. Rev. Chem. Biomol. Eng.* 3, 29–54. doi:10.1146/annurev-chembioeng-062011-081108
- Wang, M., Liu, C., Xu, X., and Li, Q. (2016). Theoretical Study of the Pyrolysis of Vanillin as a Model of Secondary Lignin Pyrolysis. *Chem. Phys. Lett.* 654, 41–45. doi:10.1016/j.cplett.2016.03.058
- Yerrayya, A., Natarajan, U., and Vinu, R. (2019). Fast Pyrolysis of Guaiacol to Simple Phenols: Experiments, Theory and Kinetic Model. *Chem. Eng. Sci.* 207, 619–630. doi:10.1016/j.ces.2019.06.025
- Zhao, Y., and Truhlar, D. G. (2008). Density Functionals with Broad Applicability in Chemistry. *Acc. Chem. Res.* 41, 157–167. doi:10.1021/ar700111a

Conflict of Interest: The authors declare that the research was conducted in the absence of any commercial or financial relationships that could be construed as a potential conflict of interest.

Publisher's Note: All claims expressed in this article are solely those of the authors and do not necessarily represent those of their affiliated organizations, or those of the publisher, the editors and the reviewers. Any product that may be evaluated in this article, or claim that may be made by its manufacturer, is not guaranteed or endorsed by the publisher.

Copyright © 2022 Yerrayya, Natarajan and Vinu. This is an open-access article distributed under the terms of the Creative Commons Attribution License (CC BY). The use, distribution or reproduction in other forums is permitted, provided the original author(s) and the copyright owner(s) are credited and that the original publication in this journal is cited, in accordance with accepted academic practice. No use, distribution or reproduction is permitted which does not comply with these terms.